Biophysical Letter

3D-SIM Super-resolution of FtsZ and Its Membrane Tethers in *Escherichia coli* Cells

Veronica Wells Rowlett[1] and William Margolin[1,*]
[1]Department of Microbiology and Molecular Genetics, University of Texas Medical School at Houston, Houston, Texas

ABSTRACT FtsZ, a bacterial homolog of eukaryotic tubulin, assembles into the Z ring required for cytokinesis. In *Escherichia coli*, FtsZ interacts directly with FtsA and ZipA, which tether the Z ring to the membrane. We used three-dimensional structured illumination microscopy to compare the localization patterns of FtsZ, FtsA, and ZipA at high resolution in *Escherichia coli* cells. We found that FtsZ localizes in patches within a ring structure, similar to the pattern observed in other species, and discovered that FtsA and ZipA mostly colocalize in similar patches. Finally, we observed similar punctate and short polymeric structures of FtsZ distributed throughout the cell after Z rings were disassembled, either as a consequence of normal cytokinesis or upon induction of an endogenous cell division inhibitor.

Received for publication 16 May 2014 and in final form 21 August 2014.

*Correspondence: william.margolin@uth.tmc.edu

The assembly of the bacterial tubulin FtsZ has been well studied in vitro, but the fine structure of the cytokinetic Z ring it forms in vivo is not well defined. Super-resolution microscopy methods including photoactivated localization microscopy (PALM) and three-dimensional-structured illumination microscopy (3D-SIM) have recently provided a more detailed view of Z-ring structures. Two-dimensional PALM showed that Z rings in *Escherichia coli* are likely composed of loosely-bundled dynamic protofilaments (1,2). Three-dimensional PALM studies of *Caulobacter crescentus* initially showed that Z rings were comprised of loosely bundled protofilaments forming a continuous but dynamic ring (1–3). However, a more recent high-throughput study showed that the Z rings of this bacterium are patchy or discontinuous (4), similar to Z rings of *Bacillus subtilis* and *Staphylococcus aureus* using 3D-SIM (5). Strauss et al. (5) also demonstrated that the patches in *B. subtilis* Z rings are highly dynamic.

Assembly of the Z ring is modulated by several proteins that interact directly with FtsZ and enhance assembly or disassembly (6). For example, FtsA and ZipA promote ring assembly in *E. coli* by tethering it to the cytoplasmic membrane (7,8). SulA is an inhibitor of FtsZ assembly, induced only after DNA damage, which sequesters monomers of FtsZ to prevent its assembly into a Z ring (9). Our initial goals were to visualize Z rings in *E. coli* using 3D-SIM, and then examine whether any FtsZ polymeric structures remain after SulA induction. We also asked whether FtsA and ZipA localized in patchy patterns similar to those of FtsZ.

We used a DeltaVision OMX V4 Blaze microscope (Applied Precision, GE Healthcare, Issaquah, WA) to view the high-resolution localization patterns of FtsZ in *E. coli* cells producing FtsZ-GFP (Fig. 1). Three-dimensional views were reconstructed using softWoRx software (Applied Precision). To rule out GFP artifacts, we also visualized native FtsZ from a wild-type strain (WM1074) by immunofluorescence (IF).

Both FtsZ-GFP (Fig. 1, *A*, *B*, and *B*1) and IF staining for FtsZ (Fig. 1, *C*, *D*, and *D*1) consistently localized to patches around the ring circumference, similar to the *B. subtilis* and *C. crescentus* FtsZ patterns (4,5). Analysis of fluorescence intensities (see Fig. S1, *A* and *B*, in the Supporting Material) revealed that the majority of Z rings contain one or more gaps in which intensity decreases to background levels (82% for FtsZ-GFP and 69% for IF). Most rings had 3–5 areas of lower intensity, but only a small percentage of these areas had fluorescence below background intensity (34% for FtsZ-GFP and 21% for IF), indicating that the majority of areas with lower intensity contain at least some FtsZ.

To elucidate how FtsZ transitions from a disassembled ring to a new ring, we imaged a few dividing daughter cells before they were able to form new Z rings (Fig. 1 *E*). Previous conventional microscopy had revealed dynamic FtsZ helical structures (10), but the resolution had been insufficient to see further details. Here, FtsZ visualized in dividing cells by 3D-SIM localized throughout as a mixture of patches and randomly-oriented short filaments (*asterisk* and *dashed oval* in Fig. 1, respectively). These structures may represent oligomeric precursors of Z ring assembly.

To visualize FtsZ after Z-ring disassembly another way, we overproduced SulA, a protein that blocks FtsZ assembly. We examined *E. coli* cells producing FtsZ-GFP after

Editor: Sean Sun.

http://dx.doi.org/10.1016/j.bpj.2014.08.024

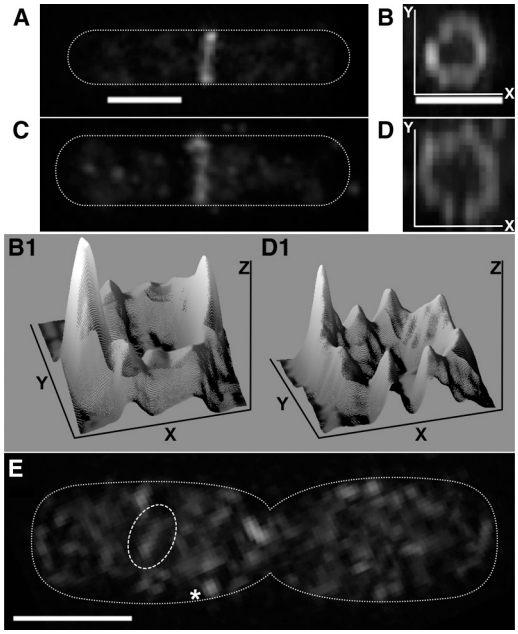

FIGURE 1 Localization of FtsZ in *E. coli*. (*A*) Cell with a Z ring labeled with FtsZ-GFP. (*B*) Rotated view of Z ring in panel *A*. (*C*) Cell with a Z ring labeled with DyLight 550 (Thermo Fisher Scientific, Waltham, MA). (*D*) Rotated view of Z ring in panel *C*. (*B*1 and *D*1) Three-dimensional surface intensity plots of *Z* rings in panels *B* and *D*, respectively. (*E*) A dividing cell producing FtsZ-GFP. The cell outline is shown in the schematic. (*Asterisk*) Focus of FtsZ localization; (*open dashed ovals*) filamentous structures of FtsZ. Three-dimensional surface intensity plots were created using the software ImageJ (19). Scale bars, 1 μm.

induction of *sulA* expression from a pBAD33-*sulA* plasmid (pWM1736) with 0.2% arabinose. After 30 min of *sulA* induction, Z rings remained intact in most cells (Fig. 2 *A* and data not shown). The proportion of cellular FtsZ-GFP in the ring before and after induction of *sulA* was consistent with previous data (data not shown) (1,11).

Notably, after 45 min of *sulA* induction, Z rings were gone (Fig. 2, *B* and B1), replaced by numerous patches and randomly-oriented short filaments (*asterisk* and *dashed ovals* in Fig. 2), similar to those observed in a dividing cell. FtsZ normally rapidly recycles from free monomers to ring-bound polymers (11), but a critical concentration of SulA reduces the pool of available FtsZ monomers, resulting in breakdown of the Z ring (9). The observed FtsZ-GFP patches and filaments are likely FtsZ polymers that disassemble before they can organize into a ring.

We confirmed this result by overproducing SulA in wild-type cells and detecting FtsZ localization by IF (Fig. 2, *C*, *D*, and *D*1). The overall fluorescence patterns in cells producing FtsZ-GFP versus cells producing only native FtsZ were similar (Fig. 2, *B*1 and *D*1), although we observed fewer filaments with IF, perhaps because FtsZ-GFP confers slight resistance to SulA, or because the increased amount of FtsZ in FtsZ-GFP producing cells might titrate the SulA more effectively.

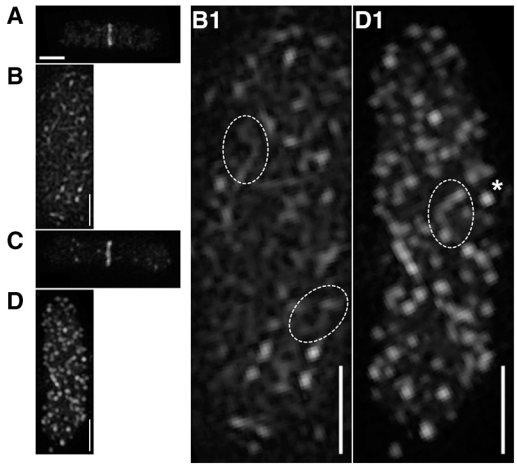

FIGURE 2 Localization of FtsZ after overproduction of SulA. (*A*) Cell producing FtsZ-GFP after 0.2% arabinose induction of SulA for 30 min. (*B*) After 45 min. (*B*1) Magnified cell shown in panel *B*. (*C*) Cell producing native FtsZ labeled with AlexaFluor 488 (Life Technologies, Carlsbad, CA) 30 min after induction; (*D*) 45 min after induction. (*D*1) Magnified cell shown in panel *D*. Scale bars, 1 μm. (*Asterisk*) Focus of FtsZ localization; (*open dashed ovals*) filamentous structures of FtsZ.

Additionally, we wanted to observe the localization patterns of the membrane tethers FtsA and ZipA. Inasmuch as both proteins bind to the same C-terminal conserved tail of FtsZ (12–14), they would be expected to colocalize with the circumferential FtsZ patches in the Z ring. We visualized FtsA using protein fusions to mCherry and GFP (data not shown) as well as IF using a wild-type strain (WM1074) (Fig. 3 *A*). We found that the patchy ring pattern of FtsA localization was similar to the FtsZ pattern. ZipA also displayed a similar patchy localization in WM1074 by IF (Fig. 3 *B*).

To determine whether FtsA and ZipA colocalized to these patches, we used a strain producing FtsA-GFP (WM4679) for IF staining of ZipA using a red secondary antibody. FtsA-GFP (Fig. 3 *C*) and ZipA (Fig. 3 *D*) had similar patterns of fluorescence, although the three-dimensional intensity profiles (Fig. 3, *C*1 and *D*1) reveal slight differences in intensity that are also visible in a merged image (Fig. 3 *E*). Quantitation of fluorescence intensities around the circumference of the rings revealed that FtsA and ZipA colocalized almost completely in approximately half of the rings analyzed (Fig. 3 *F*, and see Fig. S2 *A*), whereas in the other rings there were significant differences in localization in one or more areas (see Fig. S2 *B*). FtsA and ZipA bind to the same C-terminal peptide of FtsZ and may compete for binding. Cooperative self-assembly of FtsA or ZipA might result in large-scale differential localization visible by 3D-SIM.

In conclusion, our 3D-SIM analysis shows that the patchy localization of FtsZ is conserved in *E. coli* and suggests that it may be widespread among bacteria. After disassembly of the Z ring either in dividing cells or by excess levels of the cell division inhibitor SulA, FtsZ persisted as patches and short filamentous structures. This is consistent with a highly

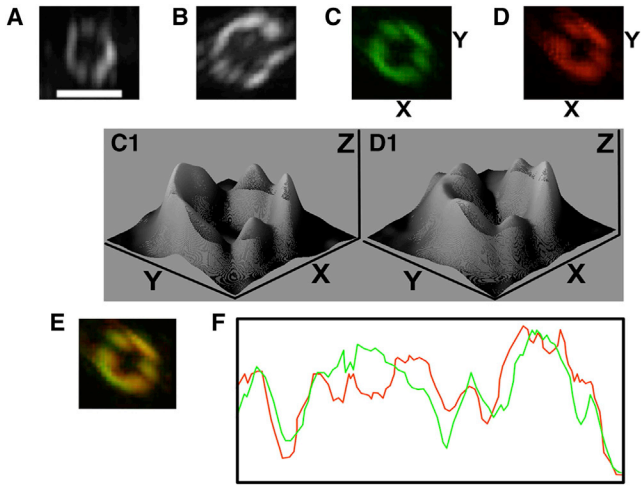

FIGURE 3 Localization of FtsA (*A*) and ZipA (*B*) by IF using AlexaFluor 488. (*C*) FtsA-GFP ring. (*D*) Same cell shown in panel *C* with ZipA labeled with DyLight 550. (*C*1 and *D*1) Three-dimensional surface intensity plots of FtsA ring from panel *C* or ZipA ring from panel *D*, respectively. (*E*) Merged image of FtsA (*green*) and ZipA (*red*) from the ring shown in panels *C* and *D*. (*F*) Intensity plot of FtsA (*green*) and ZipA (*red*) of ring shown in panel *E*. The plot represents intensity across a line drawn counterclockwise from the top of the ring around the circumference, then into its lumen. Red/green intensity plot and three-dimensional surface intensity plots were created using the software ImageJ (19). Scale bar, 1 μm.

dynamic population of FtsZ monomers and oligomers outside the ring, originally observed as mobile helices in *E. coli* by conventional fluorescence microscopy (10) and by photoactivation single-molecule tracking (15). FtsA and ZipA, which bind to the same segment of FtsZ and tether it to the cytoplasmic membrane, usually display a similar localization pattern to FtsZ and each other, although in addition to the differences we detect by 3D-SIM, there are also likely differences that are beyond its ~100-nm resolution limit in the *X*,*Y* plane.

As proposed previously (16), gaps between FtsZ patches may be needed to accommodate a switch from a sparse Z ring to a more condensed ring, which would provide force to drive ring constriction (17). If this model is correct, the gaps should close upon ring constriction, although this may be beyond the resolution of 3D-SIM in constricted rings. Another role for patches could be to force molecular crowding of low-abundance septum synthesis proteins such as FtsI, which depend on FtsZ/FtsA/ZipA for their recruitment, into a few mobile supercomplexes.

How are FtsZ polymers organized within the Z-ring patches? Recent polarized fluorescence data suggest that FtsZ polymers are oriented both axially and circumferentially within the Z ring in *E. coli* (18). The seemingly random orientation of the non-ring FtsZ polymeric structures we observe here supports the idea that there is no strong constraint requiring FtsZ oligomers to follow a circumferential path around the cell cylinder. The patches of FtsZ in the unperturbed *E. coli* Z ring likely represent randomly oriented clusters of FtsZ filaments that are associated with ZipA, FtsA, and essential septum synthesis proteins. New super-resolution microscopy methods should continue to shed light on the in vivo organization of these protein assemblies.

SUPPORTING MATERIAL

Preparation of Samples for 3D-SIM and two figures are available at http://www.biophysj.org/biophysj/supplemental/S0006-3495(14)00895-9.

ACKNOWLEDGMENTS

We thank Anna and Tomasz Zal for training on the OMX V4 Blaze system and technical suggestions.

This work was supported by National Institutes of Health grant No. GM61074 and the Graduate School of Biomedical Sciences.

SUPPORTING CITATIONS

Reference (20) appears in the Supporting Material.

REFERENCES and FOOTNOTES

1. Fu, G., T. Huang, …, J. Xiao. 2010. In vivo structure of the *E. coli* FtsZ-ring revealed by photoactivated localization microscopy (PALM). *PLoS ONE.* 5:e12682.
2. Buss, J., C. Coltharp, …, J. Xiao. 2013. In vivo organization of the FtsZ-ring by ZapA and ZapB revealed by quantitative super-resolution microscopy. *Mol. Microbiol.* 89:1099–1120.
3. Biteen, J. S., E. D. Goley, …, W. E. Moerner. 2012. Three-dimensional super-resolution imaging of the midplane protein FtsZ in live *Caulobacter crescentus* cells using astigmatism. *ChemPhysChem.* 13:1007–1012.
4. Holden, S. J., T. Pengo, …, S. Manley. 2014. High throughput 3D super-resolution microscopy reveals *Caulobacter crescentus* in vivo Z-ring organization. *Proc. Natl. Acad. Sci. USA.* 111:4566–4571.
5. Strauss, M. P., A. T. F. Liew, …, E. J. Harry. 2012. 3D-SIM super resolution microscopy reveals a bead-like arrangement for FtsZ and the division machinery: implications for triggering cytokinesis. *PLoS Biol.* 10:e1001389.
6. Romberg, L., and P. A. Levin. 2003. Assembly dynamics of the bacterial cell division protein FtsZ: poised at the edge of stability. *Annu. Rev. Microbiol.* 57:125–154.
7. Pichoff, S., and J. Lutkenhaus. 2002. Unique and overlapping roles for ZipA and FtsA in septal ring assembly in *Escherichia coli*. *EMBO J.* 21:685–693.
8. Pichoff, S., and J. Lutkenhaus. 2005. Tethering the Z ring to the membrane through a conserved membrane targeting sequence in FtsA. *Mol. Microbiol.* 55:1722–1734.
9. Chen, Y., S. L. Milam, and H. P. Erickson. 2012. SulA inhibits assembly of FtsZ by a simple sequestration mechanism. *Biochemistry.* 51:3100–3109.
10. Thanedar, S., and W. Margolin. 2004. FtsZ exhibits rapid movement and oscillation waves in helix-like patterns in *Escherichia coli*. *Curr. Biol.* 14:1167–1173.
11. Anderson, D. E., F. J. Gueiros-Filho, and H. P. Erickson. 2004. Assembly dynamics of FtsZ rings in *Bacillus subtilis* and *Escherichia coli* and effects of FtsZ-regulating proteins. *J. Bacteriol.* 186:5775–5781.
12. Ma, X., and W. Margolin. 1999. Genetic and functional analyses of the conserved C-terminal core domain of *Escherichia coli* FtsZ. *J. Bacteriol.* 181:7531–7544.

13. Szwedziak, P., Q. Wang, …, J. Löwe. 2012. FtsA forms actin-like protofilaments. *EMBO J.* 31:2249–2260.

14. Mosyak, L., Y. Zhang, …, W. S. Somers. 2000. The bacterial cell-division protein ZipA and its interaction with an FtsZ fragment revealed by x-ray crystallography. *EMBO J.* 19:3179–3191.

15. Niu, L., and J. Yu. 2008. Investigating intracellular dynamics of FtsZ cytoskeleton with photoactivation single-molecule tracking. *Biophys. J.* 95:2009–2016.

16. Lan, G., B. R. Daniels, …, S. X. Sun. 2009. Condensation of FtsZ filaments can drive bacterial cell division. *Proc. Natl. Acad. Sci. USA.* 106:121–126.

17. Osawa, M., and H. P. Erickson. 2011. Inside-out Z rings—constriction with and without GTP hydrolysis. *Mol. Microbiol.* 81:571–579.

18. Si, F., K. Busiek, …, S. X. Sun. 2013. Organization of FtsZ filaments in the bacterial division ring measured from polarized fluorescence microscopy. *Biophys. J.* 105:1976–1986.

19. Schneider, C. A., W. S. Rasband, and K. W. Eliceiri. 2012. NIH image to ImageJ: 25 years of image analysis. *Nat. Methods.* 9:671–675.

20. Levin, P. A. 2002. Light microscopy techniques for bacterial cell biology. *In* Methods in Microbiology, Vol. 31: Molecular Cellular Microbiology. P. Sansonetti and A. Zychlinsky, editors. Academic Press, London, United Kingdom, pp. 115–132.

SUPPORTING MATERIAL

3D-SIM Super-Resolution of FtsZ and its Membrane Tethers in *Escherichia coli* cells

Veronica Wells Rowlett and William Margolin

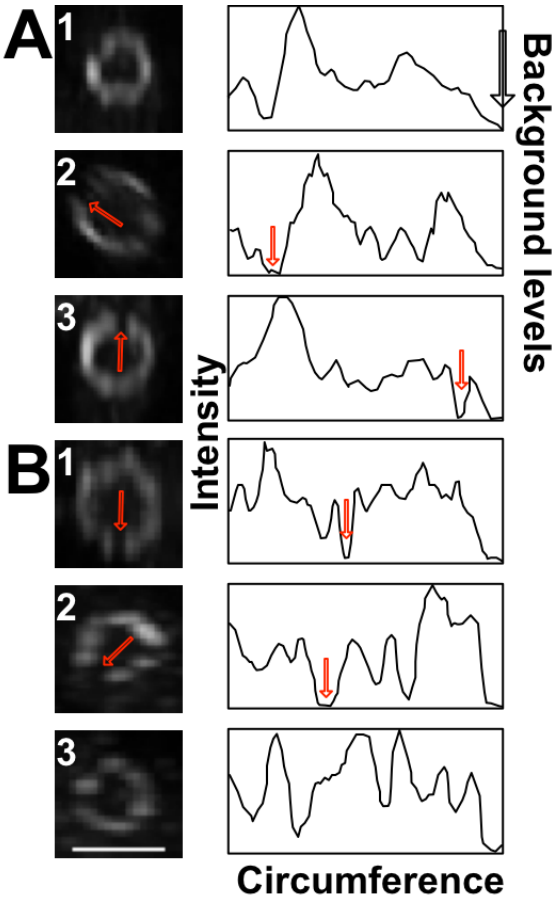

FIGURE S1 Quantitation of fluorescence intensities around the circumference of Z rings. (A) Three representative examples of FtsZ-GFP ring cross-sections and their fluorescence intensities. The plots on the right represent fluorescence intensities along a line originating at the top of the ring drawn counterclockwise around the entire circumference of the Z ring, with a final extension of the line into the lumen of the ring to define the background fluorescence intensity, shown at the far right of the plots (denoted by large arrow). Red arrows indicate areas of fluorescence intensity that are at or below background levels; areas of the ring corresponding to these areas are shown with arrows in the images on the left. (B) Three representative examples of the intensity of Z rings detected by immunofluorescence. Plots and arrows are as described above. Intensity measurements were generated using ImageJ (1) and traced in Pixelmator. Scale bar, 1 µm.

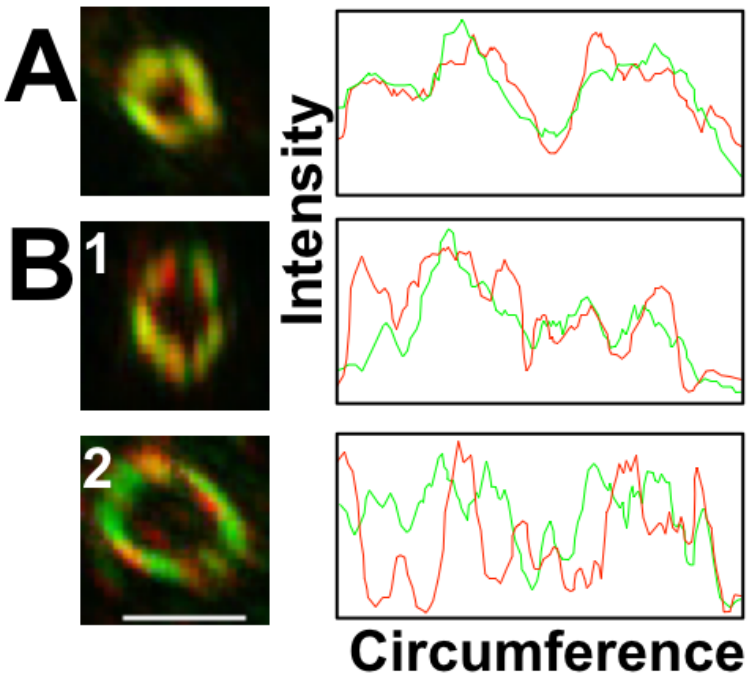

FIGURE S2 Quantitation of FtsA and ZipA colocalization. WM4769 cells producing FtsA-GFP were fixed and stained to detect ZipA localization using a red secondary antibody. (A) An example of FtsA and ZipA colocalization (another is shown in Fig. 3E-F), measured by plotting RGB intensities along a line originating at the top of the ring drawn counterclockwise around the entire circumference of the ring, with a final extension of the line into the lumen of the ring to define background intensity (far right of plot). The green line represents FtsA localization and the red line represents ZipA localization. (B) Two representative examples of colocalization patterns that have one (B1) or more (B2) significant differences in localization. RGB plots are as described above. RGB plots were generated using ImageJ (1) and traced in Pixelmator. Scale bar, 1 µm.

SUPPORTING METHODS

Preparation of samples for 3D-SIM

Cells producing FtsZ tagged with green fluorescent protein (GFP) in strain WM2026 were grown to mid-logarithmic phase, fixed using glutaraldehyde and paraformaldehyde (2), adhered to poly-lysine coated coverslips and inverted onto a drop of either ProLong Gold (Life Technologies) or Vectashield mounting medium (Vector Laboratories). Strain WM2026 harbors the native *ftsZ* gene along with a *ftsZ-gfp* gene fusion located elsewhere in the chromosome under control of an isopropyl β-D-1-thiogalactopyranoside (IPTG)-inducible *trc* promoter. To produce FtsZ-GFP as a dilute label less than the level of native FtsZ, 30 μM IPTG was added to cultures 3 h prior to fixation.

Wild-type cells (WM1074) were grown and fixed as described above, then treated with lysozyme followed by washes and incubation with affinity-purified anti-FtsZ as described (2), with the following modifications. Fixed cells were adhered to poly-lysine coated coverslips instead of a 15-well slide. The coverslips were washed by immersion in 1X phosphate-buffered saline (PBS) followed by soaking for 10 min in 1X PBS in a small container. Blocking buffer and diluted antibodies were spotted onto parafilm and coverslips were inverted onto the spots.

SUPPORTING REFERENCES

1. Schneider, C.A., W.S. Rasband, and K.W. Eliceiri. 2012. NIH Image to ImageJ: 25 years of image analysis. *Nat. Meth*. 9: 671-675.
2. Levin, P.A. 2002. Light microscopy techniques for bacterial cell biology. *In* Methods in Microbiology, Vol. 31: *Molecular Cellular Microbiology*. P. Sansonetti and A. Zychlinsky, editors. Academic Press Ltd., London, United Kingdom. 115-132.